RECOVERING OVER/UNDER-EXPOSED REGIONS IN PHOTOGRAPHS

LIKUN HOU[†], HUI JI[†], AND ZUOWEI SHEN[†]

Abstract. When taking pictures using a commodity camera in a scene with strong or harsh lighting, such as a sunny day outdoors, we often see a loss of highlight details (*over-exposure*) in some bright regions and a loss of shadow details (*under-exposure*) in some dark regions. In this paper, we developed a wavelet tight frame based approach to reconstruct a well-exposed image with better visibility on details from the one with over/under-exposed regions. There are two modules in the proposed approach: one in lightness channel that in-paints the clipped lightness and adjustes image contrast; and the other in chromatic channels that in-paints the saturated colour regions. The experiments showed that our method can effectively repair over/under-exposed regions and it performed better than other existing methods on tested real photographs.

Key words. image in-painting, contrast enhancement, wavelet, tight frame, sparse approximation

AMS subject classifications. 68U10, 65J22,65T60

1. Introduction. In digital photography, *exposure* controls how much light can reach the image sensor and the lightness of a photograph is determined by the amount of light shown. There is a physical limitation on the lightness contrast that a camera can capture, term as *dynamic range*. An outdoor scene with strong or harsh lighting often has a much wider dynamic range than the bearing capacity of a regular image sensor, which then will lead to a loss of highlight/shadow details in the resulting photograph. For example, the dynamic range of a regular digital camera is about $10^3 : 1$ while the dynamic range of an outdoor scene in a sunny day ranges from 10^5 to $10^9 : 1$. When recording such a high dynamic range (HDR) scene using a commodity camera with low dynamic range (LDR), some bright parts of the scene would be recorded as "white" which is described as *over-exposure*; and some dark areas with interesting details would be indistinguishable from"black" in the image which is described as *under-exposure*. In other words, the lightness values of those over-exposed pixels are clipped at the maximum value ($= 1$) such that these pixels only show white colour, as the values of three colour channels (red, green, blue) at these pixels are also the maximum value. Similarly, the lightness values of under-exposed pixels are too small, close to the minimum value ($= 0$), such that the image details can hardly be visually perceived. See Figure 1.1 for an illustration of two photographs with over-exposed and under-exposed regions.

Fig. 1.1: Sample real photographs with over/under-exposed regions.

1.1. Problem Formulation. In a quick glance, it seems that over-exposure correction can be classified as some existing image restoration task. For example, one might treat it as a

[†]Department of Mathematics, National University of Singapore, 10, Lower Kent Ridge Road, Singapore 119076

regular image in-painting problem, and then use some existing image in-painting approach to directly recover the details of over-exposed regions. Most existing colour in-painting methods usually recover the missing colour information of over-exposed pixels from their neighbouring regions or from some global self-similarities. However, the overall brightness of the in-painted over-exposed regions will then be in general similar to that of their neighbouring well-exposed regions. As a result, the local contrast and the reflection in the repaired over-exposed area look very artificial and the picture does not appear to be taken from a realistic lighting condition, since the over-exposed regions are supposed to be brighter than their neighbouring regions. See Figure 1.2 (b) for an illustration.

(a) (b) (c) (d)

Fig. 1.2: Demonstration of over-exposure correction using two regular colour image processing techniques and using the specifically designed one. (a) The input photograph; (b) the result by in-painting the over-exposed regions using the wavelet-based in-painting method [5]; (c) the result by enhancing the image contrast using the contrast enhancement method [30]; (d) the result from the proposed method.

Another quick solution is to directly apply some colour contrast enhancement technique to reduce over/under-exposure. However, there are a few drawbacks when doing so. For example, the missing chromatic information is not recovered on those over-exposed regions. Also, the dynamic range allowed in LDR images often is not effectively utilized in the results, as contrast enhancement tends to compress the dynamic range. See Figure 1.2 (c) for an illustration.

As we can see from Figure 1.2, the generic colour image restoration techniques are not optimized to correct over/under-exposure in digital photography. There is certainly a need to develop special colour image restoration method for correcting over/under-exposure. In recent years, there have been a few colour image restoration methods specifically designed for over-exposure correction; see e.g. [37, 29, 23]. Both methods from [37] and [29] are designed for recovering 'partial over-exposure', i.e. the colour of over-saturated regions is not completely white. They are not applicable to correcting over-exposed regions with completely white colour. The correction of fully over-exposed regions is firstly considered by Guo *et al.* in [23] by processing three colour channels in CIELAB space using different strategies. Let $[L; a; b]$ represents the lightness value and two chromatic values of the colour (see e.g. [24]). The over-exposure correction in Guo *et al.* [23] is done by (i) running a dynamic range compression in the lightness channel L; and (ii) running an in-painting method in the two chromatic channels $[a; b]$ to recover the missing chromatic information. It is noted that lowering the lightness of the over-exposed region is a necessary step in order to show vivid colour, as the colour appear white when L is close to the maximum value 1.

The experiments done in Guo *et al.* [23] showed better performance than many generic colour restoration methods. However, there are still plenty of room for further improvement. Firstly, the lightness channel of the result is not fully utilized by compressing the low dynamic

range. Secondly, the dynamic range compression technique used in [23] is directly copied from the tone mapping technique proposed in [20], which is designed for re-mapping the high dynamic range of an HDR image to a low dynamic range. Such a tone mapping technique often erases shadow details of under-exposed regions. Lastly, the recovery of image details of the over-exposed regions by [23] is not very satisfactory.

1.2. Basic idea and our contribution. In this paper, we propose an approach for correcting over/under-exposure in photographs. Our approach considers the simultaneous correction of both over-exposed and under-exposed regions, since they are often co-existing for the scenes with very high dynamic range (see Figure 1.1 for an illustration). Different from [23], we propose to decompose the problem of over/under-exposure correction into the following three sub-problems:

1. an in-painting problem of recovering clipped values of over-exposed regions in lightness channel L;
2. a lightness adjustment problem of fitting the in-painted lightness into the range allowed in LDR images without losing shadow details;
3. an in-painting problem of recovering chromatic details of over-exposed regions in two chromatic channels $[a; b]$.

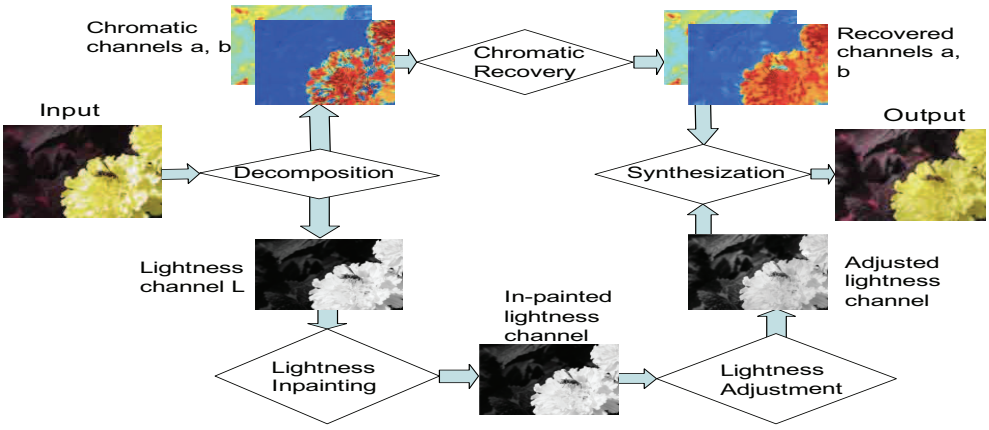

Fig. 1.3: Workflow of the proposed method.

The first sub-problem is about how to recover the lightness values of over/under-exposed pixels which are clipped to fit the range $[0, 1]$. After the recovery, the range of the lightness channel will be slightly larger than the physical range $[0, 1]$ (see Figure 3.5 (d)). Then, the sequent sub-problem is about how to adjust the lightness of the whole image to fit the physical range while revealing more image details of dark regions. Recall that the colour of over-exposed regions is completely white since their lightness values are set to the maximum $(= 1)$. Then, the last sub-problem is about how to recover the missing colour details of over-exposed pixels from the information of their neighbouring well-exposed pixels.

Based on the proposed formulation, we developed a wavelet tight frame based approach to correct over/under-exposure. See Figure 1.3 for the illustration of the proposed workflow. There are three main components in our method:

(i) a wavelet frame based regularization procedure for recovering clipped lightness of over-saturated regions.

(ii) a lightness adjustment procedure that simultaneously fits the recovered lightness into the range $[0, 1]$ and improves the contrast of under-exposed lightness without amplifying image noise.
(iii) a wavelet frame based regularization method for recovering the missing chromatic details of over-exposed regions in two chromatic channels.

The proposed approach is applicable to any photograph with both fully over-exposed regions and severely under-exposed regions. There are several advantages of the proposed method over the existing ones, including more effective use of lightness range, better recovery of chromatic details in over-exposed regions, and better local contrast of the under-exposed regions.

2. Preliminaries and related work. Over/under exposure happens when the dynamic range of a scene is higher than the dynamic range supported by the camera. As a result, the colour information of the over-exposed regions is completely lost by only showing white colour. Similarly, the colour information of the under-exposed regions is hardly perceived by showing nearly black colour. Colour correction is a challenging task, as the human perception of colour is a very profound process which is still not fully understood yet. In the past, many techniques have been developed to solve various types of colour restoration problems. In the next, we give a very brief review on some related colour image restoration techniques with a particular focus on image contrast enhancement and image in-painting.

2.1. Image contrast enhancement and image in-painting. The brightness values of over exposed pixels are clipped due to the limitation of dynamic range of LDR images. By assuming that for each over-exposed region, there is likely to exist some well-exposed region similar to the over-exposed one, Wang *et al.* [36] used some texture synthesis technique to recover the missing details of the over-exposed regions. Their approach requires the manual input of well-exposed regions that match over-exposed regions. Rempel *et al.* [32] proposed an approach to recover the lightness of a picture by fitting the brightness of an over-exposed region and its neighbourhood using a smooth function. This method is mainly for recovering the lightness and the chromatic details are not recovered.

Another technique related to brightness adjustment is image contrast enhancement, a technique that eliminates the effect of non-uniform illumination while preserving image details. Many image contrast enhancement methods have been proposed in the past. One popular approach is based on the so-called *histogram equalization* (see e.g. [21, 25]). The basic idea is to adjust image intensities so that the most frequent intensity values can be well spread out. This allows the areas of low contrast to gain a higher contrast. The histogram equalization based methods tend to work better on the images whose foreground and background are either both bright or both dark. They are not suitable to the images with both dark and bright regions. Another popular approach is the so-called *Poisson image editing* [31] which can be used for tone mapping, contrast enhancement, shade removal and etc. The basic idea is approximating the given image in some image gradient domain to reduce the effect of non-uniform illuminance while keeping fine details. Poisson image editing either can be done via solving an ℓ_2 norm related minimization (see e.g. [30]) or can be done via applying some local gradient compression operator on the image (see e.g. [20]).

Due to the saturation of brightness channel of over-exposed regions, the chromatic information of those over-exposed pixels is completely lost. The recovery of chromatic information can be viewed as an in-painting process. There have been an abundant literature on image in-painting, which is first proposed by [28] to repair damaged pixels in the image from un-damaged pixels. There are many representative image in-painting approaches. One is the PDE-based variational approach which propagates information available from un-damaged pixels to damaged pixels in the direction of the isophotest (see e.g. [3, 4]). One is treating the

image in-painting problem as a linear inverse problem and solve it via some regularization methods. For example, the TV (total variation) based regularization (see e.g. [11, 12]) and the wavelet tight frame based regularization (see e.g. [5, 9, 18]) have been used for general image in-painting. Another one is the template-based approach which covers the image patches of the damaged regions by using the similar patches of undamaged regions (see e.g. [15, 16]).

2.2. Existing methods designed for over-exposure correction. There are few methods specifically designed for over-exposure correction. The earlier work assumes that only 'partial over-exposure' occurs in an input photograph, that is, at least one colour channel is not fully saturated among all three colour channels: red, green and blue. Zhang and Brainard [37] estimated the global ratios among three colour channels using well-exposed regions of the image. Then the saturated colour channel of over-exposed regions is recovered by applying the estimated ratio on two un-saturated channels. Masood *et al.* [29] improved the results of [37] by using a spatially varying ratio function to recover the saturated colour channel of over-posed regions. The applicability of these two approaches are limited, as all three colour channels of over-exposed regions in most photographs are often all fully saturated. Over-exposure correction for fully over-exposed regions is first considered by Guo *et al.* in [23] with a much more sophisticated approach. There are two main components in Guo *et al.*'s approach : (i) applying some tone mapping technique to compress dynamic range of the given image to make room for the recovered lightness of over-exposed regions; and (ii) estimating the colour of over-exposed pixels by image in-painting. In [23], the tone mapping technique proposed by Fattal *et al.* [20] is modified and adopted for dynamic range compression. The in-painting process in two colour channels $[a; b]$ is done via a modified version of the colourization method proposed by Levin *et al.* [26] in which the colour of the targeted pixel is propagated from its neighbouring similar pixels. The similarity of pixels are determined from their lightness and chromatic values.

Before ending this section, we give a brief introduction to wavelet tight frame, which plays an essential role in our approach. Interested readers may refer to [35] for more details.

2.3. Preliminaries on wavelet tight frame. A wavelet tight frame system ([33]) is a redundant system that generalizes the concept of orthonormal wavelet basis. The wavelet tight frame for $L_2(\mathbb{R}^d)$ starts with a finite set of generators $\Psi := \{\psi_1, \psi_2, \dots, \psi_r\} \in L_2(\mathbb{R}^d)$. The shifts and dilations of these generators define an affine system:

$$X := \{\psi_{\ell,k,j} : 1 \le \ell \le r,\ k \in \mathbb{Z}^d,\ j \in \mathbb{Z}\} \tag{2.1}$$

with $\psi_{\ell,k,j} := 2^{j/2}\psi_\ell(2^j \cdot -k)$, $\psi_\ell \in \Psi$. The affine system $X(\Psi) \subset L_2(\mathbb{R}^d)$ is called a *wavelet tight frame* of $L_2(\mathbb{R}^d)$ if it is a tight frame which satisfies the following *perfect reconstruction* property:

$$f = \sum_{x \in X} \langle f, x\rangle x, \quad \text{for any } f \in L_2(\mathbb{R}^d). \tag{2.2}$$

where $\langle \cdot, \cdot \rangle$ is the inner product of $L_2(\mathbb{R}^d)$.

As a generalization of an orthonormal basis, wavelet tight frame achieves greater flexibility than an orthonormal basis by sacrificing linear independence, while it still has the perfect reconstruction property (2.2) like an orthonormal wavelet basis does. As a result, the filters associated with an MRA-based wavelet tight frame system have several desired properties not present in those of orthonormal wavelets, e.g., symmetry (anti-symmetry), smoothness and shorter support. Moreover, same as orthonormal wavelets, wavelet tight frames have very efficient numerical schemes for signal decomposition and reconstruction, which is done via discrete convolutions and samplings.

One construction scheme of wavelet tight frame systems is using multi-resolution analysis (MRA). In 1D case, it starts with a refinable function $\phi \in L^2(\mathbb{R})$ such that $\phi(x) = 2\sum_k h_0(k)\phi(2x-k)$ for some low-pass filter h_0. Then the set of framelets is defined as $\psi_\ell(x) = 2\sum_k h_\ell(k)\phi(2x-k)$ with high-pass filters h_ℓ, $\ell = 1,\dots,r$, which satisfy the so-called *unitary extension principle* (see [33]):

$$\tau_{h_0}(\omega)\overline{\tau_{h_0}(\omega+\gamma\pi)} + \sum_{\ell=1}^{r} \tau_{h_\ell}(\omega)\overline{\tau_{h_\ell}(\omega+\gamma\pi)} = \delta_{\gamma,0}, \quad \gamma = 0,1,$$

where $\tau_h(\omega)$ is the trigonometric polynomial of the filter h defined by

$$\tau_h(\omega) = \sum_k h(k)e^{ik\omega}.$$

Then for any $f \in L^2(\mathbb{R})$, we have a multi-scale framelet decomposition of f:

$$\{c_k := \langle f, \phi(\cdot - k)\rangle; \quad d_{\ell,k,j} := \langle f, \psi_{\ell,k,j}\rangle, 1 \le \ell \le r, k \in \mathbb{Z}, j \ge 0\} \tag{2.3}$$

and f can be synthesized from these coefficients:

$$f(x) = \sum_{k\in\mathbb{Z}} c_k\phi(x-k) + \sum_{k,j\in\mathbb{Z},j\ge 0}\sum_{\ell=1}^{r} d_{\ell,k,j}\psi_{\ell,k,j}(x). \tag{2.4}$$

In the implementation of the proposed method, we use the piecewise linear spline framelet system [33], whose associate filters are as follows:

$$h_0 = \frac{1}{4}[1,2,1]^\top;\ h_1 = \frac{\sqrt{2}}{4}[1,0,-1]^\top;\ h_2 = \frac{1}{4}[-1,2,-1]^\top.$$

The 2D framelets for representing images can be obtained via the tensor product of 1D framelets. The discrete implementation of 2D framelet system used in this paper is the same as that in Cai *et al.* [5], which uses a shift-invariant multi-level tight framelet decomposition without down-sampling.

The flexibility and the redundancy of wavelet tight frame make it a better choice for many image restoration tasks than orthonormal wavelet basis, as the results from a redundant wavelet system tend to have less artifacts than those from orthonormal wavelet basis (see e.g. [14]). Moreover, given an image, it is more likely to have a sparse approximation under a wavelet tight frame system than under an orthonormal wavelet basis. Together with the recent progresses on sparse approximation under redundant system using ℓ_1 norm related minimization, wavelet tight frame has been used in many image restoration problems with impressive performance, e.g., image in-painting [5, 18] and image deblurring [9, 7, 8]. Particularly, the well-known total variation (TV) regularization and its variations (see e.g. [34, 13, 10]) are closely related to ℓ_1 norm of wavelet tight frame coefficients. It is shown in [6] that, by choosing parameters properly, the minimization using the ℓ_1 norm of wavelet tight frame coefficients as the penalty function can be seen as some sophisticated discretization of the minimization involving the TV penalties or their generalizations.

Given the tensor piecewise linear framelet system associated with $\{h_\kappa\}_{\kappa=0}^{8}$, we denote the Q-level framelet decomposition (2.3) by the rectangular matrix W, which is composed of one low-pass filtering operator W_0 at the level Q and multiple high-pass filtering operators $\{W_{\kappa,j}\}_{1\le\kappa\le 8, 1\le j\le Q}$ in a multi-scale fashion:

$$W = (W_0^\top, W_{1,Q}^\top, \dots, W_{8,Q}^\top, \dots, W_{1,1}^\top, \dots, W_{8,1}^\top)^\top. \tag{2.5}$$

where $W_{\kappa,j}$ denotes the square matrix representing the convolution operator using the high-pass filter h_κ at the scale j. Given any vector $f \in \mathbb{R}^n$, then the framelet coefficients Wf and f are related as $f = W^\top(Wf)$. In general, $W^\top W = I$ but $WW^\top \neq I$ unless the tight framelet system becomes an orthonormal system. For simplicity of discussion in the rest of this paper, we introduce the operator W_Q^h which denotes the parts of W in all high-pass channels with respect to a Q-level decomposition, i.e.,

$$W_Q^h := (W_{1,Q}^\top, \ldots, W_{8,Q}^\top, \ldots, W_{1,1}^\top, \ldots, W_{8,1}^\top)^\top.$$

Another frequently used operator is the so-called *soft thresholding* [14] operator. For each $\eta > 0$, we define the soft thresholding operator $\mathcal{T}_\eta : \mathbb{R} \mapsto \mathbb{R}$ as

$$\mathcal{T}_\eta(x) = \mathrm{sgn}(x) \cdot \max\big(|x| - \eta, 0\big), \tag{2.6}$$

and extend its definition to higher dimensional vectors by applying it on the vector element-wisely.

3. Main algorithm. In this section, we give a detailed description of the proposed approach that follows the workflow illustrated in figure 1.3. It can be seen that the lightness information and the chromatic information of pixels are processed in different modules. The main steps of our approach are outlined as follows.

Outline of the main algorithm

---

1. Converting the RGB channels of the given image I into the CIELAB channels $[L; a; b]$;
2. In-painting the lightness channel L to reconstruct a new lightness channel $\widetilde{L}$ with its values may be outside $[0, 1]$;
3. Adjusting and re-mapping the new lightness channel $\widetilde{L}$ to a new lightness channel L^* that fits the range $[0, 1]$ and the local contrast of its dark regions is enhanced.
4. In-painting the over-exposed regions in two chromatic channels $[a, b]$ to obtain two new chromatic channels $[a^*; b^*]$ that recover the missing chromatic informations of these regions.
5. Synthesizing the new colour photograph using $[L^*; a^*; b^*]$.

Among the five major steps, Step 1 and Step 5 are standard colour conversion routines between RGB colour representation and CIELAB colour representation (see [24] fore more details). The main components are Step 2, Step 3 and Step 4. The detailed discussion on Step 2 and Step 3 will be given in Section 3.1 and Section 3.2. Section 3.3 will cover the discussion of step 4 and step 5.

3.1. In-painting in lightness channel L. In an LDR photograph, the 'true' lightness values of its over-exposed pixels are clipped at the maximum value 1. As a result, the over-exposed regions become white regions without any chromatic detail. These over-exposed pixels are easily detected by checking their lightness values. In practice, the colour of the pixels whose lightness values are close to 1 is visually indistinguishable from white. Similarly, the colour of those pixels whose light values close 0 is nearly invisible. Thus we treat all pixels whose lightness values close to 1 or 0 as over/under-exposed pixels. The clipped region Γ for in-painting is then defined by

$$\Gamma := \{p : L(p) > K_1\} \bigcup \{p : L(p) < K_2\}, \tag{3.1}$$

where K_1 (close to 1), K_2 (close to 0) are two positive real numbers which determine the size of over/under exposed regions. See Figure 3.1 for an illustration of our lightness in-painting method under different settings of K_1 and K_2. Based on the contour shape of in-painted lightness region, we set $K_1 = 0.98$ and $K_2 = 0.006$ through all experiments.

The goal of this section is then to develop an in-painting method for recovering the lightness values of over/under-exposed pixels in the set Γ, the set of those pixels with lightness value close to 1 or 0. It is observed that the part associated with each clipped lightness region for in-painting usually belongs to the surface made by the same material in physical world which should have the same surface reflection property. Thus, we may assume that the change of the lightness of each individual clipped regions is smooth, as well as the transition between the clipped region and neighbouring well-exposed regions. This assumption leads to the following minimization model for the in-painting in lightness channel L:

$$\widetilde{L} = \text{argmin}_U \sum_{\kappa=1}^{8} \|W_{\kappa,1}^\top W_{\kappa,1} U\|_2^2 \tag{3.2}$$

subject to $U|_{\Gamma^c} = L|_{\Gamma^c}$, where Γ^c denote the complement of the index set Γ given in (3.1).

In the next, we give a brief explanation on the model (3.2). It is known that the wavelet frame coefficients characterize the local variations of the signal. Thus, by minimizing the wavelet coefficients of lightness channel, the solution tends to have smooth wavelet coefficients which in turn lead to lightness channel with smooth variations. The constraint is the fidelity term on the lightness value of well-posed pixels. The minimization model (3.2) is a least squares problem with linear constraints, which can be solved via solving a linear system (see [1, 2] for more details). More specifically, define $A := \sum_{\kappa=1}^{8} W_{\kappa,1}^\top W_{\kappa,1} W_{\kappa,1}^\top W_{\kappa,1}$ and B the projection matrix that maps U to $U|_{\Gamma^c}$, then there exists a vector Λ of size $|\Gamma^c|$ such that the concatenated vector $V := (L^{*\top}, \Lambda^\top)^\top$ is exactly the solution of the following linear system:

$$DX = Y, \tag{3.3}$$

where $D := \begin{bmatrix} A & B^\top \\ B & 0 \end{bmatrix}$ and $Y := \begin{bmatrix} 0 \\ L|_{\Gamma^c} \end{bmatrix}$. See Figure 3.1 for an illustration of the in-painting in lightness channel using a single-level framelet decomposition.

3.2. Lightness adjustment. The range of the lightness channel $\widetilde{L}$ recovered by solving (3.2) will be be larger than the physical range of LDR images $[0, 1]$, see Figure 3.5 (d). Thus, one needs to compress $\widetilde{L}$ to fit the range $[0, 1]$. It is noted that a simple rescaling may erase the details of the regions of low brightness. Hence, we need to simultaneously compress the lightness and enhance the contrast of under-exposed regions to keep the details. Similar to the tone mapping technique developed by Fattal *et al.* [20], we also apply some local compressing operator defined in some domain for compressing the dynamic range. More specifically, the lightness compression is done in the logarithm domain of lightness channel defined as follows:

$$\widetilde{R} := \log(\widetilde{L} + \delta), \tag{3.4}$$

where δ is some positive constant to guarantee that $\widetilde{L} + \delta > 0$. In experiments, we use

$$\delta = \begin{cases} 0.005, & \text{if } \min \widetilde{L} \geq 0; \\ -\min \widetilde{L} + 0.005, & \text{if } \min \widetilde{L} < 0. \end{cases}$$

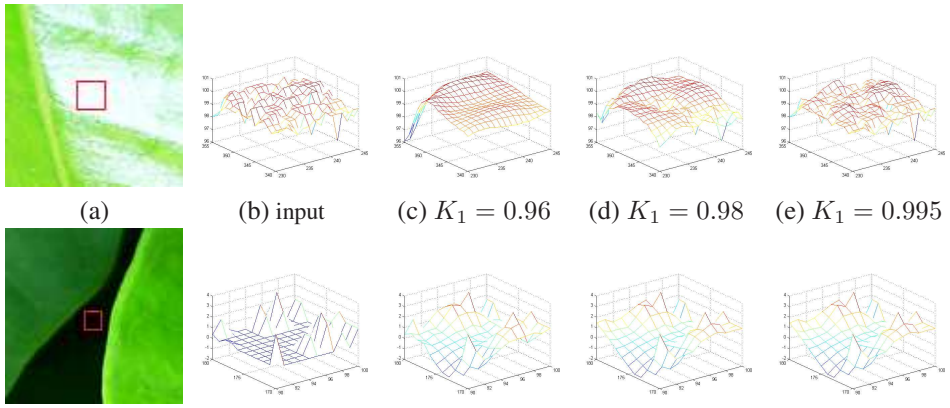

(a) (b) input (c) $K_1 = 0.96$ (d) $K_1 = 0.98$ (e) $K_1 = 0.995$

(f) (g) input (h) $K_2 = 0.002$ (i) $K_2 = 0.006$ (j) $K_2 = 0.01$

Fig. 3.1: Demonstration of lightness of over/under exposed region in-painted using different K_1 and K_2 as in (3.1). (a) The input image with over-exposed region marked out by red rectangle; (b)–(e) the contours of lightness of over-exposed region before and after in-painting; (h) the input image with under-exposed region marked out by red rectangle; (h)–(j) the contours of lightness of under-exposed region before and after in-painting. The values of K_1 and K_2 determine the sizes of regions for in-painting. The smaller(larger) the value of $K_1(K_2)$ is, the larger the region for in-painting is. As the brightness of these regions is in-painted based on the smooth prior, the large the detected region is, the smoother the in-painted brightness channel will be.

Most contrast enhancement methods for adjusting lightness channel reply on adjusting the image edges of the channel, instead of directly adjusting the intensity values. During the adjustment procedure, strong image edges and weak image edges are treated differently. The reason is that, despite the smaller magnitudes, weak image edges represent fine details. A straightforward compression will erase out these fine image details, and consequently degrade the quality of the image. Thus, to keep the visual quality of an image, an effective lightness compression method should aggressively attenuate the strength of strong image edges while conservatively attenuate the strength of weak image edges.

In our approach, we use the high-pass *wavelet tight frame* (framelet) coefficients as the measurement of image edges, as the framelet coefficients naturally encode the image gradients of different orders in a multi-scale fashion. For example, piecewise linear spline framelets capture both first-order and second-order derivative information of the image along different directions (see [6] for more details). The basic procedure of the proposed lightness adjustment is to first calculate the high-pass wavelet coefficients $W_Q^h \widetilde{R}$ for the logarithm of lightness channel R, followed by the attenuation of $W_Q^h \widetilde{R}$ by applying an attenuation function Θ on $W_Q^h \widetilde{R}$. Then the adjusted lightness channel is reconstructed by using the attenuated framelet coefficients $\Theta(W_Q^h \widetilde{R})$. See Figure 3.2 for the illustration of a flowchart of lightness adjustment. It is noted that the workflow of our proposed lightness adjustment is similar to the tone mapping technique in [20], except that ours is done in framelet domain and that one is done in finite difference domain. Another main difference between ours and the existing one lies in the design of the attenuation function, which plays an important role in the lightness adjustment. In the next, we first give a detailed discussion on the design of attenuate function, and then we present the numerical scheme of constructing lightness channel from the attenuated framelet coefficients of the logarithm of the input lightness channel.

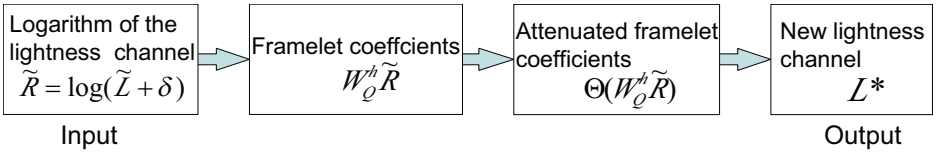

Fig. 3.2: Flowchart of the lightness adjustment procedure.

3.2.1. Design of the attenuation function Θ. The attenuation function, which we denote as Θ, plays an important role in the lightness adjustment. The function Θ in our approach takes $W_Q^h R$, i.e. the framelet coefficient of the logarithm of lightness channel, as the input. The basic principle is to attenuate more on framelet coefficients with large magnitude and attenuate less on framelet coefficients with small magnitude. For each image pixel p, a multi-scale measurement of strength of image edges centring at the pixel p is defined as

$$\vec{H}(p) = (H_1(p), H_2(p), \ldots, H_Q(p))^\top = (\|\vec{c}_1(p)\|_2, \|\vec{c}_2(p)\|_2, \ldots, \|\vec{c}_Q(p)\|_2)^\top, \quad (3.5)$$

where $\vec{c}_j$ denote the level-j high-pass framelet coefficients centering at the pixel. In other words, the j-th element of $\vec{H}(p)$ measures the overall energy of R around the pixel p in all high-pass channels at the scale 2^{j-1}, for $j = 1, 2, \ldots, Q$. It is noted that at each scale 2^{j-1}, there are totally eight high-pass channels in a piecewise linear spline framelet system which account for image gradients with different orientations and different orders. After defining the multi-scale strength measurement of image edges for each pixel p, we propose the following discrete attenuation function $\Theta : W_H^1 R \mapsto \widetilde{C_1}$ pixel-wisely that

$$\Theta\big(\vec{c}_1(p)\big) \mapsto \theta(p)\vec{c}_1(p), \quad (3.6)$$

where the weight $\theta(p)$ is some measurement of the overall strength of local image edges around the pixel p, which is defined as

$$\theta(p) = \Big[\prod_{j=1}^{Q} \frac{H_j(p)}{c' E(H_j)}\Big]^{\beta-1}, \quad (3.7)$$

where $E(H_j)$ is the average of $H_j(p)$ for all pixels p, that is, the average of the whole j-th high-pass framelet channels. There are two parameters in (3.7), $c' > 0$ and $\beta \in [0, 1]$ which control the adjustment behaviour of the lightness channel. See Figure 3.3 for an illustration of how these two parameters change the lightness channel. In our implementation, we set $\beta = 0.88$ and $c' = 0.2$ for a 3-level piecewise linear framelet decomposition (i.e. $Q = 3$ in (3.7)).

As seen from the definition of Θ in (3.7), the degree of the attenuation on each framelet coefficient depends on its magnitude. The larger is the magnitude of the frame coefficient, the more attenuation is applied on it.

3.2.2. Construction of lightness channel from the attenuated framelet coefficients. Let $\widetilde{R}$ denote the logarithm of the lightness channel L defined by (3.4) and let $W_Q^h \widetilde{R}$ denote its framelet coefficient vector. Let Θ denote the attenuation function applied on the frame coefficient vector $W_Q^h \widetilde{R}$. Then the goal is to construct a new lightness channel L^* from the attenuated framelet coefficient vector:

$$\widetilde{C_Q} = \Theta(W_Q^h \widetilde{R}) = \Theta\big(W_Q^h \log(\widetilde{L} + \delta)\big). \quad (3.8)$$

We propose to construct the new lightness channel L^* via setting

$$L^* := \exp(R^*), \tag{3.9}$$

with R^* being the solution of the following minimization problem:

$$R^* := \text{argmin}_R \frac{1}{2}\|W_1^h R - \widetilde{C_1}\|_2^2 + \eta\|W_1^h R\|_1 \tag{3.10}$$

subject to $\sum_j R(j) = \sum_j \widetilde{R}(j)$, where $\widetilde{C_1}$ denotes the attenuated single-level framelet coefficient vector given by (3.8) with $Q = 1$ and η is the regularization parameter. There are two terms in the objective function of (3.10). The first is the fidelity term and the second is the sparsity prompting regularization term on framelet coefficient vector of the solution. The ℓ_1 norm related regularization term is to suppress image noise while keeping edges sharp [9]. The reconstruction is not very sensitive to the value of regularization parameter η as long as η is reasonably small (e.g. , when $\eta \leqslant 1 \times 10^{-3}$); see Figure 3.4 for an illustration of the results using different regularization parameters. In our implementation, η is set to 5×10^{-4}. It is noted that only a single-level framelet coefficients are used for the reconstruction of the lightness channel. The main reason is that in (3.10), the reconstruction from multi-scale attenuated framelet coefficients tends to yield some undesirable effects like halos.

The adjusted lightness channel L^* obtained from (3.9) and (3.10) is usually severely squeezed. We thus re-scale it back to the physical range of the lightness channel of the original input image:

$$L^* \hookleftarrow \frac{L^* - \min(L^*)}{\max(L^*) - \min(L^*)}\big(\max(L) - \min(L)\big) + \min(L), \tag{3.11}$$

where L is the lightness channel of the original input photograph.

The minimization model (3.10) can be effectively solved by the so-called split Bregman iteration or the augmented Lagrangian method (see e.g. [22, 9]). a detailed description of the solver is given in Algorithm 1. Empirically, two parameters μ and ρ are set to be 1×10^{-3} and 5×10^{-4} respectively.

Algorithm 1. **Numerical algorithm for solving** (3.10)

---

1. Initialize $u^0, d^0, r^0,$ and c^0.
2. For $k = 0, 1, 2, \ldots$, generate u^{k+1} from u^k according to the following iteration:
   (a) $u^{k+1} \longleftarrow \arg\min_u \frac{1}{2}\|W_1^h u - C_1\|_2^2 + \frac{\mu}{2}\big\|\sum_j u(j) - \sum_j \widetilde{R}(j) + c^k\big\|_2^2 + \frac{\rho}{2}\big\|W_1^h u - d^k + r^k\big\|_2^2$;
   (b) $d^{k+1} \longleftarrow \mathcal{T}_{\eta/\rho}\big(W_1^h u^{k+1} + r^k\big)$;
   (c) $r^{k+1} \longleftarrow r^k + (W_1^h u^{k+1} - d^{k+1})$;
   (d) $c^{k+1} \longleftarrow c^k + (\sum_j u^{k+1}(j) - \sum_j \widetilde{R}(j))$;
   until $\|u^{k+1} - u^k\|_2 \leq \epsilon$ for some tolerance ϵ.
3. $R^* \longleftarrow u^{k+1}$.

The overall algorithm for in-painting and adjusting the lightness channel is summarized in Algorithm 2. See Figure 3.5 for an illustration of the changes on the overall lightness and the distribution of lightness values.

Algorithm 2. **In-painting and adjustment of the lightness channel**

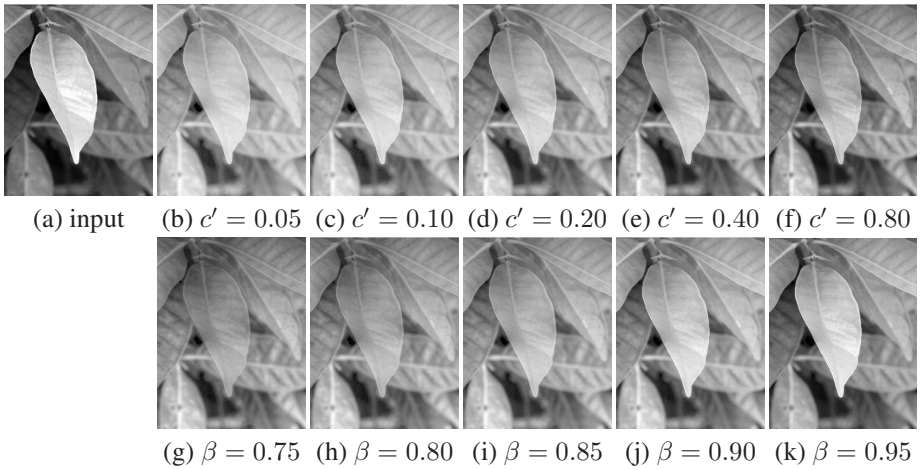

(a) input (b) $c' = 0.05$ (c) $c' = 0.10$ (d) $c' = 0.20$ (e) $c' = 0.40$ (f) $c' = 0.80$

(g) $\beta = 0.75$ (h) $\beta = 0.80$ (i) $\beta = 0.85$ (j) $\beta = 0.90$ (k) $\beta = 0.95$

Fig. 3.3: The effect on lightness adjustment when using different c' and β as in (3.7). (a) The input; (b)–(f) the results after lightness adjustment using different c' and $\beta = 0.88$; (g)–(k) the results using different β and $c' = 0.2$. The parameter c' and β are about determining the compression degree of local wavelet coefficients whose magnitude is closely related to the degree of local contrast. The value of c' determines the overall contrast change of the image. A larger value of c' will reduce the overall contrast more. The value of β determines the ratio between the boosting degree of local contrast of dark regions and the reduction degree of local contrast of bright regions. The larger the value of β is, the brighter the bright regions will be and the darker the dark regions will be.

Input: the original lightness channel L.
Output: the in-painted and adjusted lightness channel L^*
Steps:

1. Constructing the in-painted lightness channel $\widetilde{L}$ from L by solving (3.2).
2. Converting $\widetilde{L}$ to its logarithm $\widetilde{R}$ via (3.4) and computing the associated framelet coefficients $W_1^h\widetilde{R}$.
3. Adjusting the framelet coefficients $W_1^h\widetilde{R}$:
   (a) Defining the pixel-wise attenuation weights θ as (3.7) using a $Q(=3)$-level framelet decomposition $W_3^h\widetilde{R}$;
   (b) Computing adjusted framelet coefficients $\Theta(W_1^h\widetilde{R})$ by applying Θ on $W_1^h\widetilde{R}$ as in (3.6).
4. Reconstructing a new lightness channel L^* from adjusted coefficients $\Theta(W_1^h\widetilde{R})$:
   (a) Constructing R^* from $\Theta(W_1^h\widetilde{R})$ by solving (3.10), and then taking exponential of R^* to get the adjusted lightness channel L^*;
   (b) Re-scaling the values of the adjusted lightness channel L^* as in (3.11).

3.3. Recovering the chromatic channels [*a, b*]. Clearly, for those over-exposed pixels as defined by (3.1) in Section 3.1, both chromatic channels $[a; b]$ are saturated such that the original chromatic information is erased. It becomes an in-painting problem in two chromatic channels of how to recover the erased chromatic information. Similar to the in-painting approach in the lightness channel stated in Section 3.1, the pixels for recovery are first identified and then they are recovered by an in-painting process.

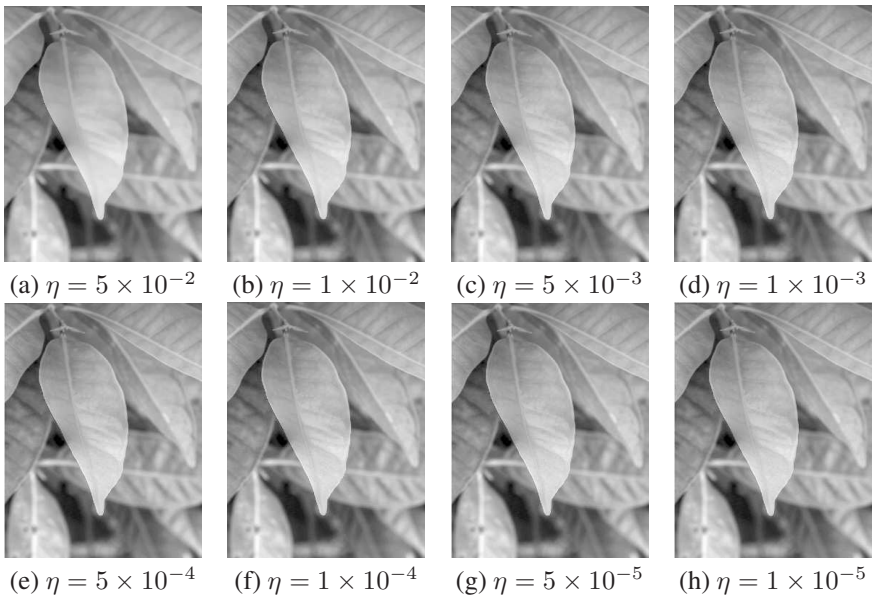

(a) $\eta = 5 \times 10^{-2}$ (b) $\eta = 1 \times 10^{-2}$ (c) $\eta = 5 \times 10^{-3}$ (d) $\eta = 1 \times 10^{-3}$

(e) $\eta = 5 \times 10^{-4}$ (f) $\eta = 1 \times 10^{-4}$ (g) $\eta = 5 \times 10^{-5}$ (h) $\eta = 1 \times 10^{-5}$

Fig. 3.4: The results of lightness reconstruction with different η as in (3.10). The value of η is closely related to the signal-to-noise ratio of the input. The lower the signal-to-noise ratio is, the larger the value of η should be set in order to suppress more noise. As a result, some image details of low contrast may be erased as well, which then leads to a result with some missing details. Thus, when the image is of good quality with high signal-to-noise ratio, the value of η should be set small in order to keep all details.

The strategy of defining pixels for recovery in two chromatic channels is slightly different from that in the lightness channel. The visual perception of colour in human is very complicated. A slight change in two chromatic channels may lead to a fairly large change in human colour perception. Thus, to avoid some rapid changes along the boundary between the over-exposed regions and the well-exposed regions, one good approach is to define a super-set of pixels for recovery. In other words, the set of pixels for recovery contains not only those over-exposed pixels, but also all pixels whose lightness are of sufficiently large magnitude and whose chromatic values are sufficiently small. Moreover, similar to [23], the assignment of pixels for recovery is done in a soft manner, instead of the hard manner as (3.1). More specifically, pixels for chromatic recovery should be

(i) of hight lightness intensity close to 1,
(ii) of inadequate chromatic information, i.e., $[a, b]$ both close to 0.

Based on the above argument, the likeliness measure of a pixel p being a pixel for recovery in two chromatic channels is defined by the following measurement as proposed in [23]:

$$M(p) = \frac{1}{2}\Big(\tanh\big(\frac{1}{60}(100 \cdot (L(p) - \ell_0) + (c_0 - \sqrt{a^2(p) + b^2(p)}))\big) + 1\Big), \tag{3.12}$$

where ℓ_0 and c_0 are two constants related to the values along the boundary of over-exposed region we defined. Same as [23], the values of ℓ_0 and c_0 are set empirically to be 0.80 and 40 respectively in (3.12) in implementations. A pixel p is defined as a pixel for recovery in two chromatic channels if $M(p) > \tau$ for some pre-defined positive constant $\tau \in (0, 1)$, so

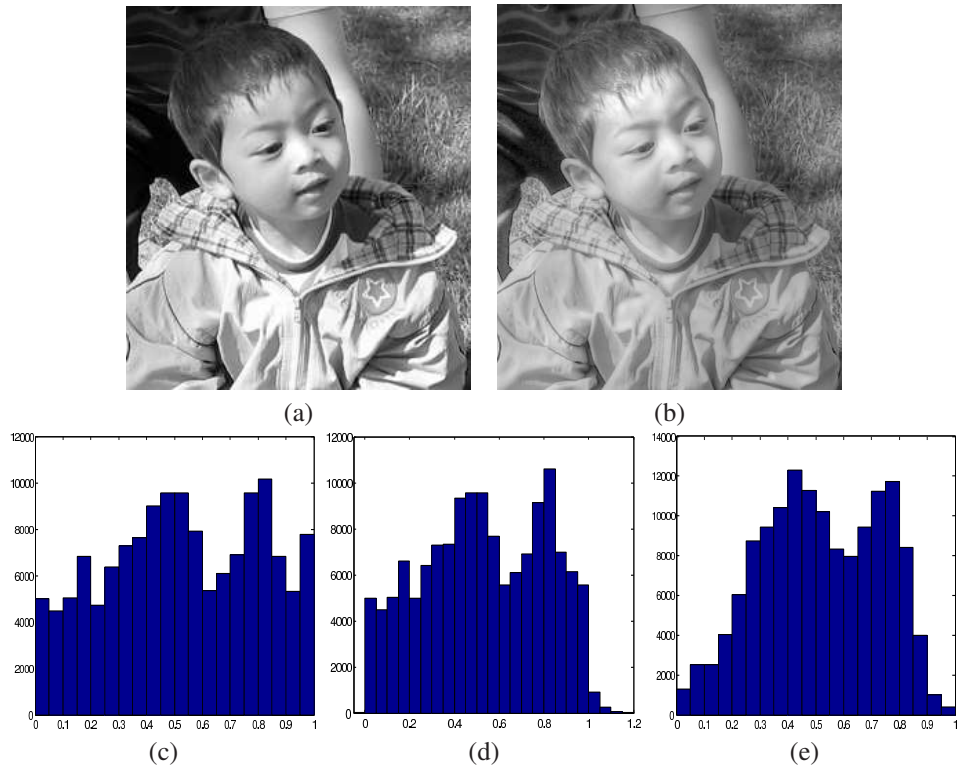

Fig. 3.5: Illustration of lightness in-painting and adjustment by Algorithm 2. (a) The input lightness channel, (b) the lightness channel after in-painting and adjustment by Algorithm 2, (c) the histogram of the input lightness channel, (d) the histogram of the lightness channel after lightness in-painting; and (e) the histogram of the lightness channel after lightness in-painting and adjustment. It can be seen from (d) that the lightness range of lightness channel is $[-0.2, 1.2]$ after applying lightness in-painting method, which goes beyond the physical range $[0, 1]$. Also, it can be seen from (e) that the pixels of lightness close to 0 or 1 are fewer in the output of Algorithm 2.

the index set of pixels for chromatic recovery is determined via

$$\Omega = \{p : M(p) > \tau\}. \tag{3.13}$$

Since the value of τ in (3.13) is to determined the over-exposed regions that need chromatic recovery, thus it cannot be very large, otherwise the over-exposed regions would not be fully covered; the value of τ cannot be very small either, otherwise the detected region for chromatic recovery would be too large and some existing chromatic details would be erased. We suggest set τ in (3.13) inside the range $[0.4, 0.7]$. See Figure 3.7 for an illustration of the results using different τ. In all experiments of this paper, we simply set $\tau = 0.5$.

The appearance of two chromatic channels of natural image is quite different from that of the lightness channel. There are much more visible variations in two chromatic channels than the lightness channel, which account for the fine details of the photograph. Motivated by the successes of sparsity prior of nature greyscale images in wavelet tight frame for various image restoration tasks (e.g. [9, 18, 8]), we propose to use the ℓ_1 norm of wavelet tight frame coefficients as the sparsity prompting functional to regularize the in-painting process. The

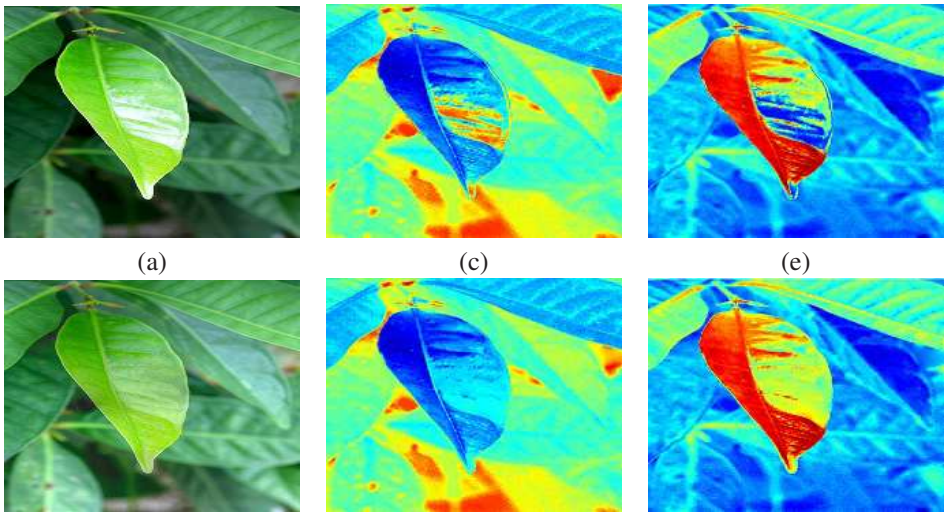

Fig. 3.6: Illustration of chromatic recovery. (a) The input photograph; (b) the synthesized photograph after lightness in-painting, adjustment and colour recovery; (c) input a-channel; (d) recovered a-channel; (e) input b-channel; (f) recovered b-channel.

following minimization model is proposed for the recovery of the chromatic channel a (the same for the recovery of the channel b):

$$a^* = \text{argmin}_u \|\text{diag}(\lambda) W u\|_1, \quad \text{subject to } u|_{\Omega^c} = a|_{\Omega^c}, \tag{3.14}$$

where Ω denotes the index set of the pixels for recovery, and Ω^c denotes its complement (see Figure 3.7). The diagonal matrix $\text{diag}(\lambda)$ is the weighting matrix whose diagonal element is determined by the likeliness measure of the corresponding pixel being saturated in the channel a. Intuitively, the larger is the likeliness measure of the pixel being saturated in the channel a, the larger the associated weight should be. Thus, the assigned weights should be monotone increasing with respect to the likeliness measure $M(p)$ as defined in (3.12). Based on the empirical observations, in our implementation, the following weighting matrix is proposed to enhance the performance

$$\lambda(c_{j,k}(p)) = (M(p) + \frac{1}{5})^2 + \frac{2}{5}.$$

To better regularize images with edges of multiple orientations, we use the wavelet tight frame system consisting of two framelet systems. One is the standard 2D tensor product of 1D piece-wise linear spline framelets; and the other is the 2D tensor product of 1D piece-wise framelets rotated by 45 degree. It is empirically observed that such a two-system tight frame system propagates the chromatic information from the well-exposed pixels to pixels for recovery better than that of a single tight frame system. The minimization (3.14) is the so-called *analysis*-based approach (see [35]), which, similar as (3.10), can also be efficiently solved by the split Bregman iteration [9].

Moreover, it is observed that a direct reconstruction of the colour photograph from the corrected $[L; a; b]$ channels will lead to some visual distortions on the colour of recovered

(a) $\tau = 0.4$ (b) $\tau = 0.5$ (c) $\tau = 0.6$ (d) $\tau = 0.7$ (e) $\tau = 0.8$ (f) $\tau = 0.9$

Fig. 3.7: Over/under-exposure correction using different τ as in (3.13). The input photograph is the one shown in Figure 3.6 (a). The value of τ determines the size of regions to be in-painted in 2 chromatic channels. The larger the value of τ is, the smaller the regions for in-painting will be, which may lead to their neighbouring un-inpainted regions remain too bright to show vivid colour, as shown in the figure.

pixels, due to the complex nature of how human perceive colour. Thus, we propose further adjustments on the two chromatic channels to keep the consistency of colour perception by normalizing the two chromatic channels as follows

$$a^* \longleftarrow \left(\frac{L^*}{L}\right)^{\frac{1}{2}} a^* \quad \text{and} \quad b^* \longleftarrow \left(\frac{L^*}{L}\right)^{\frac{1}{2}} b^*, \tag{3.15}$$

where L is the original lightness channel, L^* is the recovered lightness in (3.11). The final photograph is then synthesized from the three channels $[L^*; a^*; b^*]$. A detailed description of the numerical solver for (3.14) is given in Algorithm 3. Two parameters in Algorithm 3 are set as follows: $\mu = 0.4$ and $\rho = 0.5$. See Figure 3.6 for an illustration of the recovery of the two chromatic channels for a sample photograph.

Algorithm 3. **Numerical algorithm for recovering the chromatical channel a (b)**

1. Initialize $u^0, d^0, r^0,$ and c^0.
2. Let P_{Ω^c} denote the sample operator that only keeps the elements whose index in the set Ω^c. Then, for $k = 0, 1, 2, \ldots$, generate u^{k+1} from u^k according to the following iteration:
   (a) $u^{k+1} \longleftarrow \arg\min_u \frac{\mu}{2}\left\|P_{\Omega^c}(u-a) + c^k\right\|_2^2 + \frac{\rho}{2}\left\|Wu - d^k + r^k\right\|_2^2$;
   (b) $d^{k+1} \longleftarrow \mathcal{T}_{\lambda/\rho}\big(Wu^{k+1} + r^k\big)$;
   (c) $r^{k+1} \longleftarrow r^k + (Wu^{k+1} - d^{k+1})$;
   (d) $c^{k+1} \longleftarrow c^k + P_{\Omega^c}(u^{k+1} - a)$;
   until $\|u^{k+1} - u^k\|_2 \leq \epsilon$ for some tolerance ϵ.
3. $a^* \longleftarrow \left(\frac{L^*}{L}\right)^{\frac{1}{2}} u^{k+1}$.

In the end, the proposed approach for correcting overall over/under-exposure in photograph is summarized in Algorithm 4.

Algorithm 4. **Wavelet tight frame based method for recovering over/under-exposed regions**

1. Converting the RGB channels of the given image I into the CIELAB channels $[L; a; b]$.

2. In-painting and adjusting lightness channel L:
   (a) recovering the lightness channel $\widetilde{L}$ by in-painting the lightness values of over/under-exposed regions with clipped pixels by solving the minimization problem in (3.2);
   (b) adjusting the lightness channel $\widetilde{L}$ to obtain the contrast enhanced lightness channel L^* without losing visible image details using Algorithm 2.
3. Recovering the missing chromatic details of the over-exposed regions in two chromatic channels $[a, b]$ by solving the minimization problem in (3.14) using Algorithm 3, and as a consequence obtaining the recovered chromatic channels $[a^*, b^*]$.
4. Synthesizing the new colour photograph using the three channels $[L^*; a^*; b^*]$.

4. Numerical experiments and discussions. The proposed algorithm for correcting over/under-exposure is evaluated on several real photographs taken by a regular LDR camera. Some tested images are from [23] and [20]. Some are captured by our own using a Canon DSLR camera. The average time for processing a colour image of size 500×800 is around 3 minutes by using MATLAB (version 7.10.0) implemented on a laptop PC with Intel T9400 CPU(2.53 GHz) and 4 GB RAM.

4.1. Experimental evaluation. The proposed method is compared against several other existing methods. The methods for comparison include two existing methods specifically designed for over-exposure correction: Masood *et al.*'s method [29], Guo *et al.*'s method [23]. Moreover, to illustrate the difference between over-exposure correction and other related colour image processing problems like contrast enhancement and image in-painting, we also include the comparison to one image in-painting method and one image contrast enhancement method. The image in-painting method used in the comparison is the spline framelet based generic image in-painting method developed in [9]. The contrast enhancement technique chosen for comparison is the screened poisson equation based method proposed in [30]. All results of those methods are either directly quoted from the referenced research articles or computed from the authors' own implementations. The results are shown in Figure 4.1–4.4 for visual comparison.

In the image shown in Figure 4.1 (a), there are several over-exposed regions with very strong reflection on the leaves. It can be seen that some details are erased in the result from Masood *et al.*'s method. The colour of over-exposed regions is restored in the in-painting method [9], but the reflection of these regions is not realistic as they appear to be darker than their neighbourhoods. The contrast enhancement method [30] enhances the visibility of the regions of low contrast, but the colour of the over-exposed regions is not fixed. Overall, Guo *et al.*'s method and our method do a better job on correcting over-exposure with more realistic reflection. But the result of Guo *et al.*'s method appear to be a little bit too dark such that the visibility of the regions of low contrast becomes worse. The reason is that the dynamic range compression procedure in Guo *et al.*'s method tends to narrow the brightness range of the image. Our method does not have this problems and the result looks well-exposed on over-exposed regions and the under-exposed regions have good contrast.

In the image shown in Figure 4.2 (a), several petals are over-exposed and the background is under-exposed. Both Masood *et al.*'s method and the contrast enhancement method did not correct the over-exposed regions well. The colour of these over-exposed regions still appears to be severely whitened. In the result produced by the in-painting method [9], the damaged chromatic information is partially recovered. However, the colour still does not appear to be correct, due to the wrongly used local reflection on those repaired regions. Guo

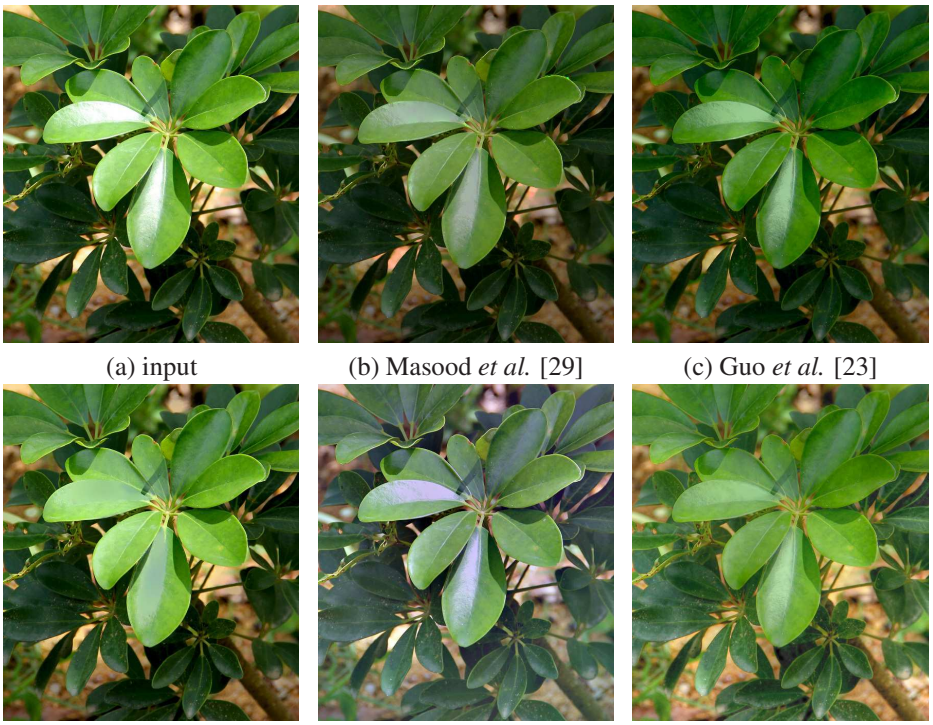

(a) input (b) Masood *et al.* [29] (c) Guo *et al.* [23]

(d) image in-painting [9] (e) contrast enhancement [30] (f) our result

Fig. 4.1: Results of different methods for processing the 'plant' example.

et al.'s method and ours both recover the damaged chromatic information in the over-exposed regions with the correct colour, but Guo *et al.*'s method did not perform correctly on under-exposed regions. The overall contrast of our result is better balanced than that from Guo *et al.*'s method. The results shown in Figure 4.3 and Figure 4.4 are consistent with what we have observed in Figure 4.1 and Figure 4.2.

In summary, the experiments show that over/under-exposure correction is a very specific colour image restoration problem. The generic colour image processing technique cannot correct the over-exposure in a satisfying manner. The image in-painting method can recover colour information, but the lack of brightness modification leads to unrealistic local reflections. The image colour enhancement can effectively improve the local contrast of under-exposed regions, but the colour of over-exposed regions is not fixed. Overall, the methods specifically designed for over/under-exposure correction, such as Guo *et al.*'s method and ours, do a better job on over/under-exposure correction. Ours is more effective on utilizing the full lightness range allowed in LDR images, and it also can effectively improve the local contrast of under-exposed regions while Guo *et al.*'s method usually decreases it.

4.2. Conclusions and future work. In this paper, we present a new wavelet frame based approach for correcting pixels that are affected by over- and under-exposure in an input photograph. Numerical results on real photographs show that our algorithm can more efficiently improve the visual quality of both over-exposed and under-exposed regions of the input photograph than some existing methods. There are still a few issues remaining when dealing with certain types of over-exposure. One is chromatic aberration occurring near the boundary

(a) input image from [23] (b) Masood *et al.* [29] (c) Guo *et al.* [23]

(d) image in-painting [9] (e) contrast enhancement [30] (f) our result

Fig. 4.2: Results of different methods for processing the 'flower' example.

of over-exposed regions (see Figure 4.5). In the proposed approach, these aberrated values might be propagated into the over-exposed regions during the chromatic recovery procedure, consequently unfaithful colourized result might be produced. Another issue is the small halo-like artifacts shown in the image with over-exposure. There is no mechanism in our approach that will remove these halo-like artifacts. In the future, we will examine how to develop more robust recovery procedure to handle chromatic aberration and suppress halo-like artifacts in a photograph with over/under-exposure.

Acknowledgements. The authors would like to thank the editor and two anonymous reviewers for their helpful and constructive comments that greatly contributed to improving the final version of this paper. The work is supported in part by the Singapore MOE AcRF Tier 2 Research Grant MOE2011-T2-1-116 and Tier 1 Research Grant R-146-000-165-112.

REFERENCES

[1] M. S. Bazaraa, H. D. Sherali and C. M. Shetty. Nonlinear Programming: Theory and Algorithms. John Wiley & Sons, 2nd edition, 1993.
[2] D. P. Bertsekas. Nonlinear Programming. Athena Scientific, 2nd edition, 1999.
[3] M. Bertalmio, G. Sapiro, V. Caselles, C. Ballester, *Image inpainting*, in *SIGGRAPH*, 417–424, 2000
[4] M. Bertalmio, L. Vese, G. Sapiro, S. Osher, Simultaneous structure and texture image inpainting, *IEEE Transactions on Image Processing* 12 (8):882–889, 2003
[5] J. Cai, R. H. Chan and Z. Shen. A framelet-based image in-painting algorithm. *Applied and Computational Harmonic Analysis*, 24:131–149, 2008.
[6] J. Cai, B. Dong, S. Osher and Z. Shen. Image restoration: total variation, wavelet frames, and beyond. *Journal of the American Mathematical Society*, 25 (4):1033–1089, 2012.
[7] J. Cai, H. Ji, C. Liu and Z. Shen. Blind motion deblurring from a single image using sparse approximation, *Proc. CVPR*, 2009.
[8] J. Cai, H. Ji, C. Liu and Z. Shen. Framelet based blind image deblurring from a single image. *IEEE Trans. Image Processing*, 21(2):562–572, 2012.
[9] J. Cai, S. Osher and Z. Shen. Split Bregman methods and frame based image restoration. *Multiscale Modeling and Simulation*, A SIAM Interdisciplinary Journal 8(2):337–369, 2009.
[10] T. F. Chan, G. Golub, and P. Mulet. A nonlinear primal-dual method for total variation-based image restoration. *SIAM Journal on Scientific Computing*, 20 (6):1964–1977, 1999.
[11] T. F. Chan and J. Shen, Mathematical models for local non-texture inpaintings, *SIAM Journal on Applied Mathematics* 62(3):1019-1043, 2002.

(a) input image from [23] (b) Masood *et al.* [29] (c) Guo *et al.* [23]

(d) image in-painting [9] (e) contrast enhancement [30] (f) our result

Fig. 4.3: Results of different methods for processing the 'child' example.

[12] T. F. Chan, J. Shen, and H. M. Zhou, Total variation wavelet inpainting, *J. Math. Imaging Vision* 25:107–125, 2006.

[13] A. Chambolle and P. Lions. Image recovery via total variation minimization and related problems. *Numerische Mathematik*, 76 (2):167–188, 1997.

[14] R. Coifman and D. Donoho. Translation-invariant de-noising. *Wavelet and Statistics*, Springer-Verlag, 103: 125–150, 1994.

[15] A. Criminisi, P. Patrick and T. Kentaro, Region filling and object removal by exemplar-based image inpainting, *IEEE Trans. Image Proc.* 13(9):1200–1212,2004.

[16] I. Drori, D. Cohen-Or and H. Yeshurun, Fragment-based image completion. In *Proc. SIGGRAPH*, 2003.

[17] P. E. Debevec and J. Malik. Recovering high dynamic range radiance maps from photographs. In *ACM SIGGRAPH*, pages 369–378, 1997.

[18] B. Dong, H. Ji, J. Li and Z. Shen. Wavelet frame based blind image in-painting. *Applied and Computational Harmonic Analysis*, 32(2):268–279, 2012.

[19] F. Durand and J. Dorsey. Fast bilateral filtering for the display of high-dynamicrange images. *ACM Transactions on Graphics*, 21(3):255–266, 2002.

[20] R. Fattal, D. Lischinski and M. Werman. Gradient domain high dynamic range compression. *ACM Transactions on Graphics* , 21(2): 249–256, 2002.

[21] P. Getreuer. Automatic colour enhancement (ACE) and its fast implementation. Image Processing On Line(IPOL), 2012.

[22] T. Goldstein and S. Osher. The split Bregman iteration for L1-regularized problems. *SIAM J. Imaging Sciences*, 2(2):323–343 2009.

[23] D. Guo, Y. Cheng, S. Zhuo and T. Sim. Correcting Over-Exposure in Photographs. *Proc. CVPR*, 2010.

[24] J. Schanda (Ed.). Colourimetry: Understanding the CIE System. John Wiley & Sons Inc., 2007.

[25] J. L. Lisani, A. B. Petro and C. Sbert. Colour and contrast enhancement by controlled piecewise affine histogram equalization. Image Processing On Line(IPOL), Preprint, 2012.

[26] A. Levin, D. Lischinski and Y. Weiss. Colourization using optimization. In *SIGGRAPH*, 2004.

[27] S. Mann and R. W. Picard. On being undigital with digital cameras: Extending dynamic range by combining

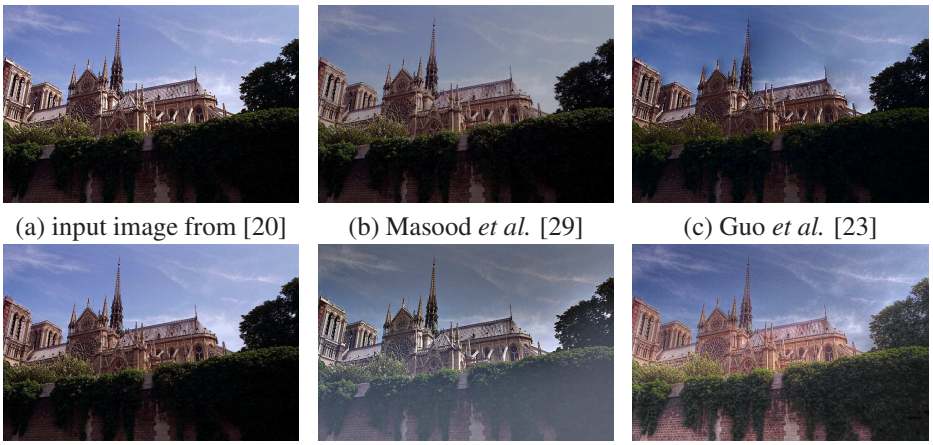

(a) input image from [20] (b) Masood *et al.* [29] (c) Guo *et al.* [23]

(d) image in-painting [9] (e) contrast enhancement [30] (f) our result

Fig. 4.4: Results of different methods for processing the 'church' example.

(a) (b)

Fig. 4.5: Demonstration of the failure in the presence of chromatic aberration by our algorithm.

differently exposed pictures, in *Proceedings of IS&T*, pages: 442–448, 1995.

[28] S. Masnou and J.-M. Morel. Level lines based disocclusion. In *Proceedings of ICIP*, pages: 259–263, 1998.

[29] S. Z. Masood, J. Zhu and M. F. Tappen. Automatic correction of saturated regions in photographs using cross-channel correlation. *Computer Graphics Forum (CGF)*, International Journal of Eurographics Association, 28(7), 2009.

[30] J. M. Morel, A. B. Petro and C. Sbert. Screened Poisson Equation for Image Contrast Enhancement. Image Processing On Line(IPOL), Preprint, 2013.

[31] P. Perez, M. Gangnet, and A. Black, Poisson image editing, *ACM Trans. Graph.*, 22(3), pages: 342–348, 003.

[32] A. Rempel, M. Trentacoste, H. Seetzen, H. Young, W. Heidrich, L. Whitehead and G. Ward. Ldr2hdr: on-the-fly reverse tone mapping of legacy video and photographs. *ACM Trans. Graph.*, 26(3), 2007

[33] A. Ron and Z. Shen. Affine systems in $L_2(\mathbb{R}^d)$: the analysis of the analysis operator. *Journal of Functional Analysis*, 148:408–447, 1997.

[34] L. Rudin, S. Osher and E. Fatemi. Nonlinear total variation based noise removal algorithms. *Phys. D*, 60:259–268, 1992.

[35] Z. Shen. Wavelet frames and image restorations. *Proceedings of the International Congress of Mathematicians*, 4:2834–2863, 2010.

[36] L. Wang, L. Wei, K. Zhou, B. Guo and H. Shum. High dynamic range image hallucination. In *EGSR*, 2007

[37] X. Zhang and D. H. Brainard. Estimation of saturated pixel values in digital colour imaging. In *J. Opt. Soc. Am. A*, 21(22): 2301–2310, 2004.